Metabolism-dependent ferroptosis promotes mitochondrial dysfunction and inflammation in CD4$^+$ T lymphocytes in HIV-infected immune non-responders

Qing Xiao,[a,b] Liting Yan,[a,c] Junyan Han,[a,d] Siyuan Yang,[a,b] Yunxia Tang,[a,b] Qun Li,[a,b] Xiaojie Lao,[a,b] Zhen Chen,[a,b] Jiang Xiao,[a,b] Hongxin Zhao,[a,b] Fengting Yu,[a,b,*] and Fujie Zhang[a,b,**]

[a]Beijing Ditan Hospital, Capital Medical University, Beijing, China
[b]Clinical Center for HIV/AIDS, Capital Medical University, Beijing, China
[c]Infectious Disease Department, Sichuan Provincial People's Hospital, University of Electronic Science and Technology of China, Chengdu, China
[d]Biomedical Innovation Center, Beijing Shijitan Hospital, Capital Medical University, Beijing, China

eBioMedicine
2022;86: 104382
Published Online XXX
https://doi.org/10.1016/j.ebiom.2022.104382

Summary

Background HIV immune non-responders (INRs) are described as a failure to reestablish a pool of CD4$^+$ T lymphocytes (CD4 cells) after antiretroviral therapy (ART), which is related to poor clinical results. Ferroptosis is a newly discovered form of cell death characterised by iron-dependent lipid peroxidation and the accumulation of reactive oxygen species (ROS). The mechanism of unrecoverable CD4 cells in INRs and whether ferroptosis plays a role are not fully understood.

Methods Ninety-two people living with HIV (PLHIVs) who experienced four-year ART with sustained viral suppression, including 27 INRs, 34 partial responders (PRs), and 31 complete responders (CRs); and 26 uninfected control participants (UCs) were analysed for 16 immune parameters with flow cytometry. Then plasma lipid, iron and oxidation, and antioxidant indicators were detected by ELISA, and CD4 cells were sorted out and visualised under transmission electron microscopy. Finally, ferroptosis inhibitors were added, and alterations in CD4 cell phenotype and function were observed.

Findings We found decreased recent thymic emigrants (RTE), over-activation and over-proliferation phenotypes, diminished killing function, decreased IL-7R and more severe inflammation; increased lipid peroxidation in the mitochondria and disruptions of the mitochondrial structure, showing typical features of ferroptosis in CD4 cells in INRs. Additionally, ferroptosis inhibitors could reduce inflammation and repair mitochondrial damage. Meanwhile, ELISA results showed increased plasma free fatty acids (FFA) and an imbalance of oxidative and antioxidant systems in INRs. Flow cytometry results displayed alterations of both transferrin receptor (CD71) and lipid transporter (CD36) expressions on the surface of CD4 cells. Mechanistically, there was a stronger correlation between CD36 expression and mitochondrial lipid peroxidation production, ferroptosis makers, and inflammation indicators; while amino acid transporter (CD98) was more related to killing functions; and CD71 was more closely related to activation status in CD4 cells.

Interpretation Cellular metabolism was closely correlated with its diverse functions in INRs. Ferroptosis was observed in CD4 cells of INRs, and inhibiting ferroptosis through modulating mitochondrial disorders and inflammation may offer an alternative immunological strategy for reinvigorating CD4 cells in INRs.

Funding This research was supported by the 13th Five-year Plan, Ministry of Science and Technology of China (2018ZX10302-102), Beijing Municipal Administration of Hospitals' Ascent Plan (DFL20191802), and Beijing Municipal Administration of Hospitals Clinical Medicine Development of Special Funding Support (ZYLX202126).

*Corresponding author. Beijing Ditan Hospital, Capital Medical University, Beijing, 100015, China.
**Corresponding author. Beijing Ditan Hospital, Capital Medical University, Beijing, 100015, China.
E-mail addresses: yufengting123@126.com (F. Yu), treatment@chinaaids.cn (F. Zhang).

Keywords: Human immunodeficiency virus (HIV); Poor immune reconstitution (PIR); Immune non-responder (INR); Ferroptosis; Metabolism; Inflammation

Research in context

Evidence before this study

Ferroptosis is an iron-dependent cell death proposed by Dr. Brent R. Stockwell in 2012. Since its introduction, a large body of literature has reported on the regulatory mechanisms of ferroptosis and its pivotal role in neurological, cancer, and metabolic settings. However, little is known about the role of ferroptosis in HIV infection and treatment. Previous studies have shown that infection of primary CD4 cells with wild-type HIV-1 reveals that HIV-infected cells exhibit more regulated cell death (RCD), including ferroptosis. Dysregulation of iron homeostasis exacerbates HIV infection, and HIV, as well as combination antiretroviral drugs, increase the risk of ferroptosis by increasing ferritin autophagy at the lysosomal level. Earlier studies have indicated a link between ferroptosis and reduced CD4 cells following HIV infection. The mechanisms by which poor immune reconstitution (PIR) occurs in HIV-1-infected patients are complex and mainly involve reduced production and excessive destruction of CD4 cells. However, no single mechanism is sufficient to fully explain the occurrence of PIR.

Added value of this study

In the present study, we detected typical ferroptosis markers, phenotypes of cell regeneration, activation, proliferation, killing, and metabolism, as well as the inflammatory status of CD4 cells in HIV immune non-responders (INRs). At the same time, we analysed the correlation between ferroptosis-associated metabolic markers and other cellular functions. We found that ferroptosis and inflammation were significantly increased in CD4 cells of INRs, and that ferroptosis inhibitors significantly reduced the levels of lipid peroxidation and inflammation in CD4 cells. The metabolic markers linked to ferroptosis were also involved in regulating other cellular functions. Specifically, iron metabolism (CD71) correlated with CD4 cell activation, amino acid metabolism (CD98) correlated with killing function, and lipid metabolism (CD36) correlated with mitochondrial lipid peroxidation, ferroptosis markers, and inflammation levels.

Implications of all the available evidence

Taken together, data from our study show decreased recent thymic emigrants, over-activated, over-proliferation and impaired killing phenotypes, disturbed mitochondrial function, increased ferroptosis, and enhanced inflammation in CD4 cells in INRs. These alterations were closely related to CD4 cell metabolism. Inhibiting ferroptosis could attenuate mitochondrial impairment and reduce the inflammatory response in CD4 cells, providing a complementary approach to the recovery of CD4 cells in INRs.

Introduction

Despite sustained viral suppression driven by adequate treatment adherence, 15–30% of HIV patients on antiretroviral therapy (ART) are immune non-responders (INRs), who are unable to rebuild a competent immune response.[1] The US Department of Health and Human Services (DHHS) treatment guidelines define that after four to seven years of ART in HIV patients, the number of $CD4^+$ T lymphocytes (CD4 cells) does not reach 350 or 500 cells/μl, which is considered poor immune reconstitution (PIR).[2] The causes for this immunological failure are complicated; mechanisms that have been identified include reduced bone marrow hematopoiesis, inadequate thymic output, residual viral replication, and disturbances in the intestinal flora. However, none of these independent factors can fully be explained.[3–7] Conversion or intense ART regimens in INRs have no effect on CD4 cell counts, and the latter are more vulnerable to AIDS-related and non-AIDS-related illness and death.[8,9] Thymic output is a pivotal process in immune reconstitution and can be inferred by assessing T cell receptor excision circles (TREC) and naive CD4 cells expressing $CD31^+$, which are termed recent thymic emigrants (RTE).[10] Previous studies have shown impaired thymic output and its links with increased CD4 cells in ART-treated people living with HIV (PLHIVs).[6,11]

Ferroptosis is a regulated cell death (RCD) caused by an excessive accumulation of iron-associated lipid peroxides in the cell and a diminished scavenging effect of glutathione peroxidase 4 (GPX4) and glutathione (GSH), which dysregulate the homeostasis of lipid reactive oxygen species (ROS) production and degradation.[12] Mitochondrial compromise and lipid peroxidation are the two most prominent features of cell ferroptosis.[13,14] When the inherent antioxidant capacity decreases and is insufficient to scavenge the excessive accumulation of ROS, oxidative-antioxidant homeostasis is disrupted, causing ferroptosis. The mitochondrial matrix and mitochondrial cristae are the main sites of oxidative metabolism in eukaryotes.[15] Mitochondria are rich in lipids and one of the most sensitive organelles to ischemia, hypoxia, and damage.[16] When cells undergo ferroptosis, electron microscopy imaging predominantly reveals shrunken and damaged mitochondria, with few additional changes visible before cell death.[12] The small

size of mitochondria with increased membrane density and vestigial cristae is the typical morphological features of ferroptosis, which do not have morphological, biochemical, or genetic characteristics with other types of regulated cell death, such as apoptosis.[6,17,18] Molecules involved in regulating iron homeostasis, lipid metabolism, and amino acid metabolism are closely related to the biological process of ferroptosis.[19] Thus, nutrient molecules involved in iron, amino acid, lipid metabolism, and various signals of lipid peroxidation are critical to the regulation of ferroptosis.[20] In the meantime, there is growing evidence that ferroptosis is associated with an inflammatory process, wherein cells release substances that significantly engage the innate immune system and control the cellular inflammatory response, signal transduction, and cell proliferation. Large quantities of proinflammatory cytokines are generated when the accumulation of lipid ROS goes beyond a particular threshold, causing the body to suffer harm,[21] but the exact threshold value of ROS is unclear. It is likely that the ferroptosis-sensibility of the cells depends on the physiological conditions, cell types, and even individual lifestyles.[22] Cell death induced by ferroptosis is tightly linked to a disturbance in redox equilibrium.[23] The downstream pathways whereby lipid peroxidation results in cell malfunction or death are not fully established, but are proposed to involve the destruction of membrane integrity, pore opening, loss of ionic homeostasis, and the production of free radicals that destroy membrane-embedded proteins necessary for cell survival.[22]

Emerging studies have reported ferroptosis in wild-type HIV-1 infected CD4 cells,[24] HIV patients with cryptococcal meningitis,[25] and HIV-associated neurocognitive disorders.[26] These patients were noted to be suffering from abnormalities in mitochondrial function. Research has also documented mitochondrial DNA (mtDNA) depletion in PLHIVs and mitochondria functional and morphological modifications in clinically stable HIV patients, which may result from HIV infection (lymphocytes) or first-line ART (monocytes).[27,28] Our team has previously discovered that HIV appears to impact mitochondrial membrane potential (MMP, $\Delta\Psi m$) in CD8 cells, causing ROS to accumulate in CD4 cells. Following ART, both cell subsets had a marked reduction in mitochondrial mass (MM), followed by a rise after three years of treatment.[29] The maintenance of MMP and MM is essential for mitochondrial function, and disorders in MMP and MM can negatively affect the redox status of factors in the respiratory chain, the distribution of ions and metabolites in the interstitial space, and thus the normal physiological function of mitochondria.[30] These findings suggest that mitochondrial abnormalities caused by both HIV infection and ART had an impact on patients' immune reconstitution. Based on the above findings, we propose a scientific hypothesis that patients with PIR may promote ferroptosis of CD4 cells through mitochondrial disturbances and thus impair immune recovery and stimulate inflammatory responses.

To test our hypothesis, we examined the expression of CD4 regeneration, cell activation, proliferation and killing markers, ferroptosis-related metabolism and mitochondrial function changes, and systemic inflammation in ART-treated PLHIVs and age-matched uninfected controls. The PLHIVs were divided into three groups based on the count of CD4 cells: immune non-responders (INRs) (≤350), partial responders (PRs) (350–500), and complete responders (CRs) (≥500).[31] We found that CD4 cells in INRs had reduced recent thymic emigrants (RTE), a greater capacity for activation and proliferation, more severe impairment of mitochondrial function and structure, more pronounced ferroptosis, and more severe inflammation than in CRs. Correlation analysis shows that the metabolism of CD4 cells is closely related to its other functions. And CD4 cells could alter lipid metabolism via controlling the expression of CD36 on the cell surface, which is involved in ferroptosis and therefore influences the body's inflammatory response and immune reconstitution. The current study describes ferroptosis in INR CD4 cells, which may help with new therapeutic strategies.

Methods

Study participants

This study was approved by the Committee of Ethics at Beijing Ditan Hospital (approval number: 2021-022-01), Capital Medical University, Beijing, China. All participants were recruited between October 2021 and March 2022, and written informed consents were obtained. The inclusion criteria for the HIV cohort were: (1) age 30–45 years old; (2) HIV-infected patients on ART for more than four years; (3) sustained virological suppression after ART and no virological failure for at least three years. And the exclusion criteria were: (1) discontinuation of ART during treatment or virological failure; (2) presence of active opportunistic infection; (3) combined hepatitis B virus (HBV), hepatitis C virus (HCV), cytomegalovirus (CMV), syphilis or other viral infections; (4) with a confirmed malignancy; (5) with severe hepatic or renal impairment. The study participants contained four populations: 92 PLHIVs on ART with undetectable viremia (HIV-RNA <40 copies/mL), consisting of 27 immune non-responders (INRs), 34 partial responders (PRs), and 31 complete responders (CRs); and 26 sex and age-matched uninfected control participants (UCs) who were negative for HIV, HBV, HCV, and other infections. The exact time of infection for these PLHIVs is unknown. The standards for INRs are: ART for at least four years, sustained virological suppression for more than three years, and CD4 cells consistently less than 350/μl for the whole treatment process. The criteria for PRs are: ART for at least four years, sustained virological suppression for more than

three years, and CD4 cells below 500/μl for the entire treatment course and consistently between 350 and 500/μl for at least one year prior to and at the time of sample collection. Moreover, the criteria for CRs are: ART for at least four years, sustained virological suppression for more than three years, and CD4 cells consistently greater than 500/μl for at least one year prior to and at the time of sample collection. The characteristics of the study participants are shown in Table 1 and Supplementary Table S1.

Blood sample collection and processing

Samples were collected after participants signed informed consent. At the time of blood collection, all participants had received ART for more than four years and reached virological suppression for at least three years. Fasting blood was collected by venipuncture in Vacutainer tubes containing EDTA (Becton Dickinson, Franklin Lakes, NJ, USA). Plasma was stored at 80 °C for further analysis, and peripheral blood mononuclear cells (PBMCs) were isolated by Lymphoprep™ (Stemcell, Vancouver, Canada, cat#07851) gradient centrifugation in SepMate™ Tubes (Stemcell, Vancouver, Canada). The cell density was determined by an automated cell counter (TC20 Automated Cell Counter, BioRad, CA, USA).

Plasma HIV viral load and cell counting

The plasma viral load was measured using Abbott RealTime HIV (m2000sp) viral load assay (Abbott Molecular, IL, USA), with a lower detection limit of 40 copies/mL. Absolute CD4 cell counts in whole blood samples were determined by standard flow cytometry on a Beckman Coulter Navios instrument (Beckman, San Jose, CA, USA).

T Cell receptor excision circle

Thymic output can be assessed by RTE or TREC measurements.[32] DNA from the PBMCs was extracted with the Nucleic Acid Isolation Kit (DAAN GENE, Guangdong, China, cat#DA0623). The TREC in PBMCs were quantified using real-time quantitative PCR (RTq-PCR) with TaqProbe 2 × qPCR-Multiplex (Sangon Biotech, Shanghai, China, cat#B630005) as described previously.[33,34] To normalise for input DNA, internal control of β-actin was amplified in every sample test, and each sample was run in duplicate. The primer and probe sequences for TREC are as follows: forward, 5′-CACATCCCTTTCAACCATGCT-3'; reverse, 5′-GCCAGCTGCAGGGTTTAGG-3'; probe, FAM-5′-ACACCTCTGGTTTTTGTAAAGGTGCCCACT-3′-TAMRA. β-actin, forward, 5′-TCACCCACACTGTGCCCATCTACGA-3′, reverse, 5′-CAGCGGAACCGCTCATTGCCAATGG-3′, probe, VIC-5′-ATGCCCTCCCCCATGCCATCCTGCGT-3′-TAMRA.

Parameters	UC	INR	PR	CR
	(n = 26)	(CD4≤350) (n = 27)	(350<CD4<500) (n = 34)	(CD4≥500) (n = 31)
Age	35 (33–38)	39 (34–43)	35 (30–40)	33 (30–40)
Sex (Male/Female)	25/1	24/3	32/2	30/1
CD4⁺ T cells (cells/mm³)	869** (555–976)	287 (229–325)	431** (398–471)	630** (565–735)
CD8⁺ T cells (cells/mm³)	641 (471–869)	549 (496–896)	665 (507–915)	759 (549–1038)
CD4/CD8 Ratio	1.34** (0.90–1.79)	0.41 (0.33–0.56)	0.68 (0.50–0.82)	0.82** (0.64–1.17)
Plasma levels of HIV RNA (copies/ml)	–	TND	TND	TND
Route of infection				
Homosexual	–	22	30	26
Heterosexual	–	3	3	3
Other	–	2	1	2
Baseline CD4⁺ T cells (cells/mm³)	–	168 (103–242)	224 (133–353)	240 (192–345)
Baseline HIV RNA (copies/ml)				
$<10^5$	–	18	26	28*
$\geq 10^5$	–	9	8	3
Treatment regimes				
TDF + EFV + 3TC		23	30	25
Others		4	4	6
Duration of ART (year)	–	5 (4.0–6.5)	5 (4.0–7.0)	6 (5.0–8.0)
Time of complete virological suppression (year)	–	4.5 (3.5–6.0)	4.5 (3.5–6.5)	5.5 (4.5–7.5)

*Represents $p < 0.05$, **represents $p < 0.01$, compared with the INR group. INRs, immune non-responders; PRs, partial responders; CRs, complete responders; TND, target not detected.

Table 1: **General characteristics of the study participants.**

Flow cytometry cell phenotype analysis

The phenotype analysis was performed by flow cytometry on freshly isolated lymphocytes. T cell phenotype was assessed using the following fluorochrome-conjugated monoclonal antibodies: anti-CD3 APC-H7 (clone SK7, RRID: AB_1645475), anti-CD4 BB515 (clone RPA-T4, RRID: AB_2744419), anti-CD4 APC (clone RPA-T4, RRID: AB_398593), anti-CD8 AF700 (clone RPA-T8, RRID: AB_396953), anti-CD45RA Percp/cy5.5 (clone HI100, RRID: AB_2738199), anti-CD71 AF647 (clone OKT9, RRID: AB_2869830), anti-CD38 PE (clone HIT2, RRID: AB_395853), anti-HLA-DR BV510 (clone G46-6, RRID: AB_2737994), anti-CD98 PE (clone UM7F8, RRID: AB_396344), anti-CD36 BV510 (clone CLB-IVC7, RRID: AB_2871606) (all from BD Biosciences, San Jose, CA); and anti-CD3 APC/Cy7 (clone SK7, RRID: AB_10644011), anti-CD4 APC (clone RPA-T4, RRID: AB_2562051), anti-CD4 FITC (clone RPA-T4, RRID: AB_2562052), anti-CD8 AF700 (clone SK1, RRID: AB_2562790), anti-CD31 PE/Dazzle 594 (clone WM59, RRID: AB_2566173) (all from Biolegend). Then PBMCs were incubated with viability dye (FVS BV510, BD Biosciences, RRID: AB_2869572) at room temperature for 15 min before being washed, or 7-AAD (percp, BD Biosciences, RRID: AB_2869266) before sample loading. Monoclonal antibodies were added for 15 min in the dark at room temperature, then washed, and events were acquired on a Beckman Coulter Navios instrument (Beckman, San Jose, CA, USA). For detection of the nuclear proteins, including Ki-67 (PE, clone B56, RRID: AB_2266296), perforin (Percp/cy5.5, clone δG9, RRID: AB_2738409), and Granzyme B (PE/Dazzle 594, clone GB11, RRID: AB_2737618), cells were surface stained as described above, fixed, and permeabilised using the Transcription Factor Buffer Set (BD Biosciences, San Jose, CA, RRID: AB_2869424), and then stained intracellular with the above-mentioned intracellular antibodies. Cryopreserved PBMCs were thawed, washed, and stained for anti-IL-7R AF647 (clone HIL-7R-M21, RRID: AB_647113). The CD4 cell gating strategy, fluorescence minus one (FMO) for all indicators, and antibody and reagent information were shown in the supplementary material (Figs. S1–S3).

Mitochondrial function test

The MMP was assessed using the JC-1 fluorescent probe (Thermo Fisher, cat# T3168), and we measured the change of the MMP based on the change of colour and calculated the ratio of monomer to the polymer to indicate the cell damage between the groups. Liperfluor was used to detect lipid ROS production (Dojindo, cat# L248). The PBMCs were stained with 5 μM Liperfluor in the dark at 37 °C for 30 min, and lipid peroxidation was determined by flow cytometry with 5 μM C11-BODIPY 581/591 (Invitrogen, cat# D3861) staining. Oxidation of a component of the C11-BODIPY fluorophore shifts the fluorescence emission from red to green, and the change in the ratio of green to red fluorescence was used as an indicator of an increase in lipid peroxidation.

In vitro stimulation and intracellular staining

To determine cytokine expression, we cultured the PBMCs (1×10^6) in RPMI medium supplemented with 10% fetal bovine serum (GIBCO, USA) and stimulated with media containing phorbol 12-myristate 13-acetate, ionomycin and brefeldin-A (Leukocyte activation cocktail with Golgiplug; BD biosciences, RRID: AB_2868893) for 4 h in 5% CO_2. The surface was stained with anti-CD3 APC-H7 (clone SK7, RRID: AB_1645475), anti-CD4 BB515 (clone RPA-T4, RRID: AB_2744419), and anti-CD8 AF700 (clone RPA-T8, RRID: AB_396953); then fixation and permeabilization were performed using the Fixation/Permeabilization Kit (BD Biosciences, RRID: AB_2869008), and intracellular staining with tumour necrosis factor-α (TNF-α) (APC, clone MAb11, RRID: AB_398566), interleukin-6 (IL-6) (PE, clone MQ2-13A5, RRID: AB_395469), interferon-γ (INF-γ) (BB700, clone B27, RRID: AB_2744484) antibodies.

CD4 cell sorting and transmission electron microscope (TEM)

PBMCs were isolated from whole blood by Ficoll density centrifugation as mentioned above. The CD4 cells were enriched from PBMCs by negative depletion ($CD4^+$ T Cell Negative Isolation Kit, Miltenyi Biotec Inc; Auburn, CA; cat# 130-096-533) following the manufacturer's instructions. Sorted $CD4^+$ T-cell subsets were on average >96% pure as determined by post-sorting Flow Cytometric analysis (Fig. S3). Sorted cells were fixed in glutaraldehyde (Servicebio, Wuhan, China, cat#G1102-100ML), and the structure of mitochondria was observed by TEM.

Ferroptosis inhibitor addition

The specific ferroptosis inhibitor Ferrostatin-1 (Fer-1, ferroptosis inhibitor; Selleck, Houston, TX, USA; cat# S7243) was used in the experiments, which was screened at different time gradients and concentration gradients. Then a cultivation concentration of 10 μM and a time of 12 h were determined (Fig. S4). The PBMCs were then incubated with 10 μM Fer-1 for 12 h, and subsequently, the mitochondrial functions, metabolic indexes, and inflammatory factors were detected as above procedures.

Enzyme-linked immunosorbent assay (ELISA)

Malondialdehyde (MDA) (TBARS Assay Kit, Cayman, MI, USA; cat#10009055), glutathione (GSH) (Glutathione Assay Kit, Cayman, cat#703002), superoxide dismutase (SOD) (Superoxide Dismutase Assay Kit,

Cayman, cat#706002), free fatty acids (FFA) (Free Fatty Acid Fluorometric Assay Kit, Cayman, cat#700310), and ferrous iron (Fe^{2+}) (Iron Colorimetric Assay Kit, Biovison, CA, USA; cat# K390) in plasma were measured by ELISA following the manual instructions. Before measurement of GSH, the plasma should be deproteinised as instructed in the manufacturer's protocol.

Statistical analysis

Acquisition and analysis of flow cytometry data were performed with Kaluza (version 2.1) and FlowJo (version 10.8.1) software. Statistical analyses were implemented using GraphPad Prism version 8.0, R version 4.0.5, SPSS version 23, and PASS version 15. The normality of each variable was assessed using the Kolmogorov–Smirnov test. Clinical characteristics of participants were analysed using the chi-square test (categorical variables) or the Kruskal–Wallis test with Dunn's multiple comparisons (continuous variables, non-parametric) and one-way analysis of variance (ANOVA) with Turkey's multiple comparisons (continuous variables, parametric). Medians and interquartile ranges were used to summarise continuous variables, and frequencies were utilised to summarise categorical variables (Table 1, Table S1). Significant factors in the univariate analysis were selected for the multivariate logistic regression analysis to identify factors independently linked with immune reconstruction (Table S2). The Kruskal–Wallis with Dunn's multiple comparisons (non-parametric, multiple comparisons) or the one-way analysis of variance (ANOVA) with Turkey's multiple comparisons (parametric, multiple comparisons) was used to analyse ELISA and flow cytometry results (Figs. 1–5). The paired Student's t-test (parametric, single comparison) or the Wilcoxon matched-pairs signed rank test (non-parametric, single comparison) was employed to compare paired variables (Fig. 6). The Spearman rank correlation test, with r representing the Spearman correlation coefficient, was used to ascertain the relationships (Figs. 1, 2, 4 and 7). It was deemed statistically significant when the $p < 0.05$ (Fig. 8).

Ethics

The study was approved by the Committee of Ethics at Beijing Ditan Hospital (approval number: 2021-022-01), Capital Medical University in Beijing, China. All participants provided written informed consent prior to enrollment.

Role of funders

The study funders had no role in the study design, data collection, data analysis, data interpretation, or writing of the report. The corresponding authors and senior authors had full access to all the data and the statistical reports.

Results

Characteristics of the participants

Twenty-six uninfected control participants (UCs) and ninety-two PLHIVs, including 27 INRs (CD4 cell count ≤350), 34 PRs (350< CD4 cell count <500), and 31 CRs (CD4 cell count ≥500), were enrolled in the study. The patient's demographic characteristics and biochemical parameters are shown in Table 1 and Supplementary Table S1. Most PLHIVs in this study contracted the infection through homosexual activity; their viral loads are currently undetectable; and they were prescribed the TDF/EFV/3TC regimen, which does not differ between groups. The current median CD4 cell counts were 869 (IQR, 555–976), 287 (IQR, 229–325), 431 (IQR, 398–471) and 630 (IQR, 565–735) cells/μl in UC, INR, PR, and CR groups; the CD4/CD8 ratio was 1.34 (IQR, 0.90–1.79), 0.41 (IQR, 0.33–0.56); 0.68 (IQR, 0.50–0.82), and 0.82 (IQR, 0.64–1.17) respectively. CD4 cell count and CD4/CD8 ratio are the lowest in the INR group, and there exist significant differences between INR and other groups. The number of patients with baseline HIV RNA>10^5 is higher in the INR group than in the CR group, suggesting that a high baseline viral load may be a risk factor for PIR (Table 1). Also, there was a significant difference in lymphocyte count, total triglycerides (TG), lactate dehydrogenase (LDH), and C-reactive protein (CRP) between INR and CR groups (Table S1). Multivariate logistic regression analysis revealed baseline HIV RNA, lymphocyte count, and TG as the independent risk factors for PIR (Table S2). However, when age, sex, baseline CD4 level, length of therapy, and duration of virological suppression were examined, no significant differences were found.

Thymic output and naive CD4 cell subsets were decreased in INRs

Regarding thymic function, we first analysed the naïve CD4 cells ($CD4^+CD45RA^+$), RTE CD4 cell subset quantifying $CD31^+$ percentage ($CD4^+CD45RA^+CD31^+$) and TREC. The naive fraction of CD4 cells was significantly lower in INRs, and the percent of $CD45RA^+CD31^+$ CD4 cells was remarkably lower in INRs than in UCs and CRs; indicating a lower frequency of RTE CD4 cells in these ART-treated PLHIVs. Noticeably, the naive CD4 cells and RTE CD4 cells in CRs were closer to UCs with no statistically significant differences (Fig. 1a and b). Moreover, the INR group showed significantly lower levels of TREC in contrast with the UC and CR groups (Fig. 1c). Correlation analysis shows there exist significant correlations between TREC (r = 0.4355), naive CD4 cell proportion (r = 0.3714), and RTE CD4 cells (r = 0.39) with CD4 cell count (Fig. 1d).

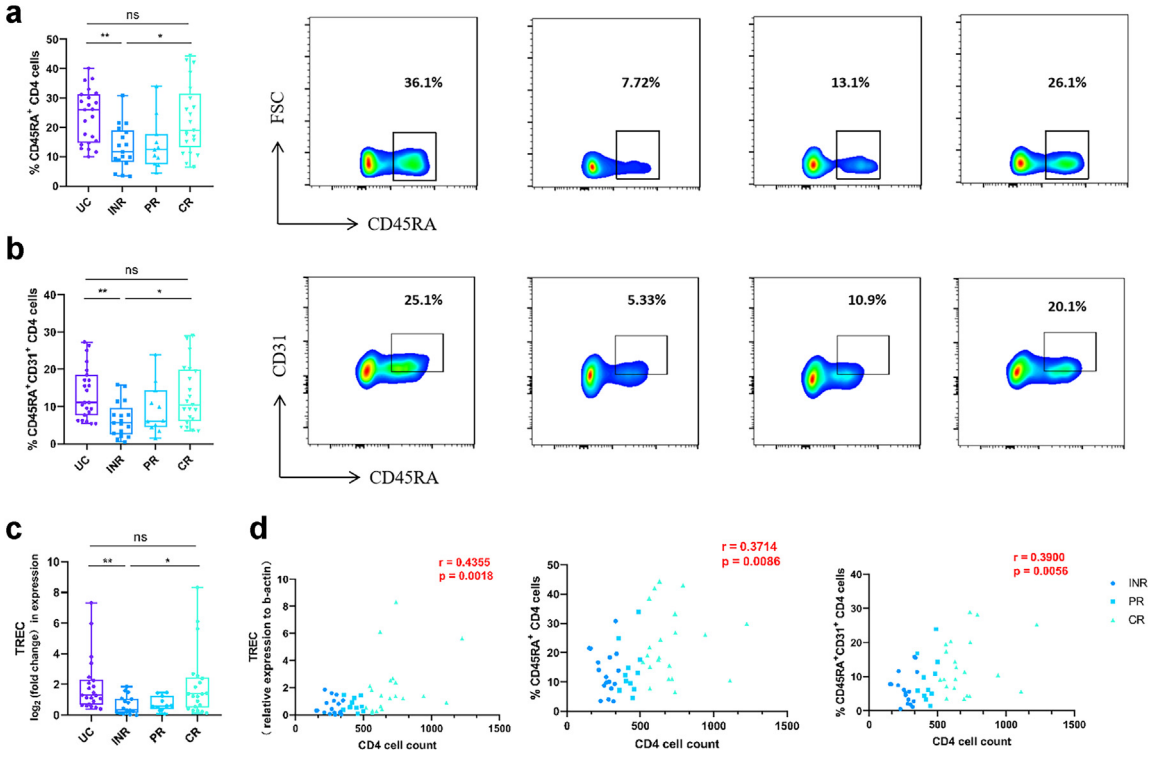

Fig. 1: **Naive CD4 cell subsets and thymic output in UCs, INRs, PRs, and CRs.** (a) Beeswarm boxplots and representative staining for CD45RA within CD4 cells in UCs, INRs, PRs, and CRs. (b) Beeswarm boxplots and representative staining for CD45RA and CD31 within CD4 cells in UCs, INRs, PRs, and CRs. (c) Correlation analysis of the percentages of naive CD4 cells, RTE naive CD4 cells and TREC with CD4 cell count in PLHIVs (UC: n = 22; INR: n = 17, PR: n = 11; CR: n = 21). *p < 0.05, **p < 0.01. UCs, uninfected control participants; INRs, immune non-responders; PRs, partial responders; CRs, complete responders; PLHIVs, people living with HIV; TREC, T cell receptor excision circles.

Alterations in CD4 cell activation, proliferation, and killing functions in INRs

We then analysed cell activation, proliferation, and killing markers in CD4 cells from UCs, INRs, PRs, and CRs. T cell activation was evaluated by assessing the percentages of $CD38^+$/$HLA\text{-}DR^+$ T cells. Fig. 2a shows that the co-expression of CD38 and HLA-DR was higher in INRs compared with UCs and CRs, suggesting that CD4 cells were activated in vivo in INRs. Simultaneously, higher frequencies of CD4 cells expressed Ki-67 in INRs than CRs and UCs, suggesting that CD4 cell proliferation is active in INRs. But this difference is relatively small between INR and PR groups (Fig. 2b). Effector lymphocytes are capable of producing lytic granules containing perforin and granzymes, which are released onto the surface of the target cells, subjecting cells to lytic necrosis.[35] We then examined the function of CD4 cell non-specific killing and found comparable levels of perforin and granzyme among INR, PR, and CR groups. However, the intracellular perforin in the INR group was considerably lower than that in the UC group, suggesting that PLHIVs had a partial impairment of the cytotoxic function of CD4 cells (Fig. 2c and d). The correlation analysis confirmed that the percentage of $CD38^+HLA\text{-}DR^+$ ($r = -0.41$, $p < 0.0001$) and $Ki\text{-}67^+$ ($r = -0.28$, $p = 0.0065$) cells negatively related to CD4 count, and the correlation of $perforin^+$ cells was just the opposite ($r = 0.22$, $p = 0.0319$). However, we could not find a correlation between the Granzyme B^+ CD4 cells and CD4 counts ($r = 0.15$, $p = 0.1486$) (Fig. 2e). Taken together, these results suggest that CD4 cells in PLHIVs exhibit features of T-cell pluripotency that correlate with immune reconstitution.

CD4 cells are prone to ferroptosis and mitochondrial dysfunction in INRs

The process of ferroptosis is often characterised by mitochondrial malfunction and lipid peroxidation due to ROS buildup as mitochondria are essential to cellular survival and functioning[36]; we next examined essential mitochondrial functions in CD4 cells. We performed staining for JC-1 to detect changes of MMP. When the MMP is depolarised, JC-1 is present as a monomer and fluoresces green. The results showed that the proportion of MMP decreased in INRs was significantly higher than in the other three groups, and that MMP was

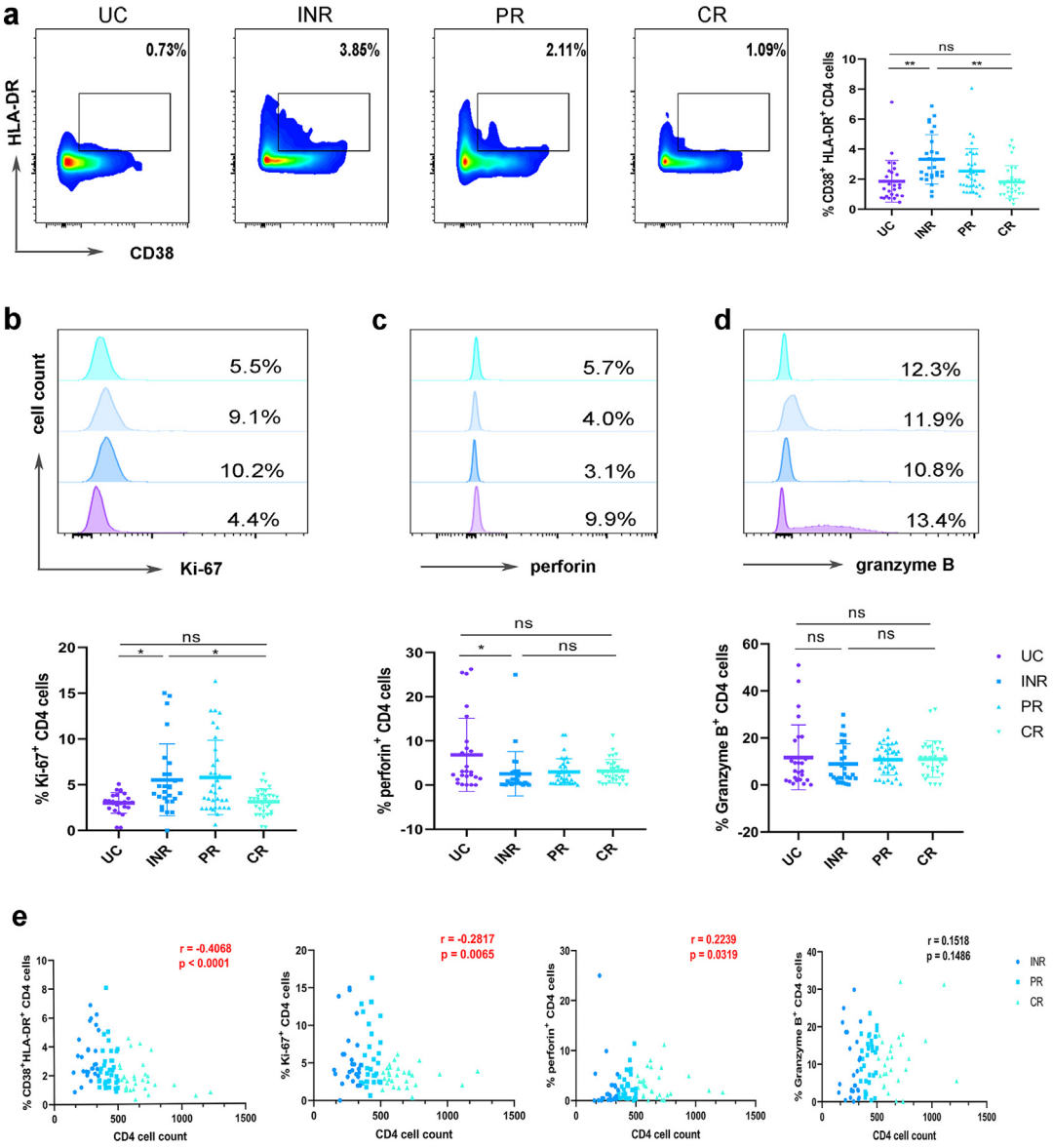

***Fig. 2:* Proportion of CD4 cell activation, proliferation, and killing markers and their association with CD4 cell count.** (a) Representative staining and beeswarm boxplots for CD38 and HLA-DR within CD4 cells from UCs, INRs, PRs, and CRs. (b) The expression of Ki-67, (c) perforin, and (d) granzyme B were represented as histograms (upper) and beeswarm boxplots (lower) comparing median frequency in CD4 cells among UCs, INRs, PRs, and CRs. (e) Correlation analysis of the percentages of $CD38^+HLA\text{-}DR^+$, $Ki\text{-}67^+$, $perforin^+$, and granzyme B^+ cells with CD4 cell count in PLHIVs (UC: n = 26; INR: n = 27, PR: n = 34; CR: n = 31). *p < 0.05, **p < 0.01. UCs, uninfected control participants; INRs, immune non-responders; PRs, partial responders; CRs, complete responders; PLHIVs, people living with HIV.

increased in both the PR and CR groups to varying degrees (Fig. 3a).

Lipid peroxidation is a fundamental mechanism of ferric cell death, and we next measured lipid ROS and lipid peroxidation. The results showed that the level of ROS in the INR group was significantly higher than in the other three groups. In contrast, the ROS level in the CR group was comparable to those in the PR group, but both were higher than that in the UC group (Fig. 3b). Meanwhile, cellular lipid peroxidation was the highest in INRs, alleviated in PRs and CRs. And lipid peroxidation levels were lower in CRs than PRs, but higher than UCs (Fig. 3c). There have been reports of alterations in mitochondrial structure occurring concurrently with ferroptosis due to the close relationship between mitochondrial function and morphology. We observed mitochondrial atrophy, reduced or even

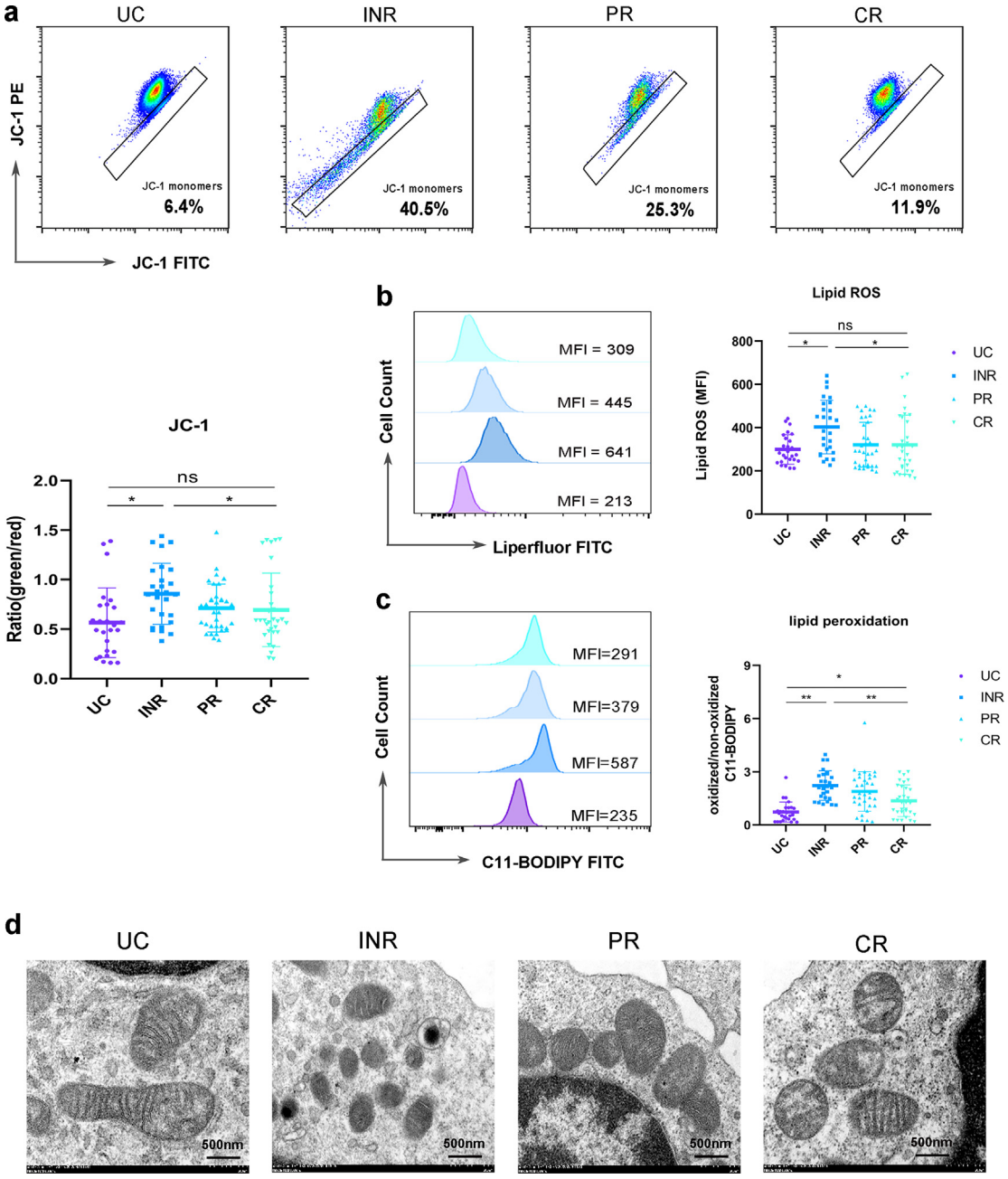

***Fig. 3:* CD4 cell mitochondrial functions and structures.** (a) Representative staining (upper) and beeswarm boxplots (lower) for JC-1 (green/red) within CD4 cells from UCs, INRs, PRs, and CRs. (b) Intracellular ROS levels were represented as histograms (left) and beeswarm boxplots (right) in UCs, INRs, PRs, and CRs. (c) Intracellular lipid peroxidation levels and the ratio of oxidised to non-oxidised C11-BODIPY were represented separately as histograms (left) and beeswarm boxplots (right) in UCs, INRs, PRs, and CRs. (d) Typical transmission electron microscope images of sorted CD4 cells in UCs, INRs, PRs, and CRs (UC: n = 26; INR: n = 27, PR: n = 34; CR: n = 31). *p < 0.05, **p < 0.01. UCs, uninfected control participants; INRs, immune non-responders; PRs, partial responders; CRs, complete responders, MFI, median fluorescence intensity.

absent mitochondrial ridges, and increased membrane density in INRs through TEM compared with UCs. And mitochondrial structural disorders were slightly improved in PRs in contrast with IRs. Meanwhile, CRs had significantly larger mitochondrial sizes, clear mitochondrial ridge structures, and reduced membrane density than INRs. These results demonstrate increased lipid peroxidation and increased levels of cellular ferroptosis in CD4 cells of INRs (Fig. 3d).

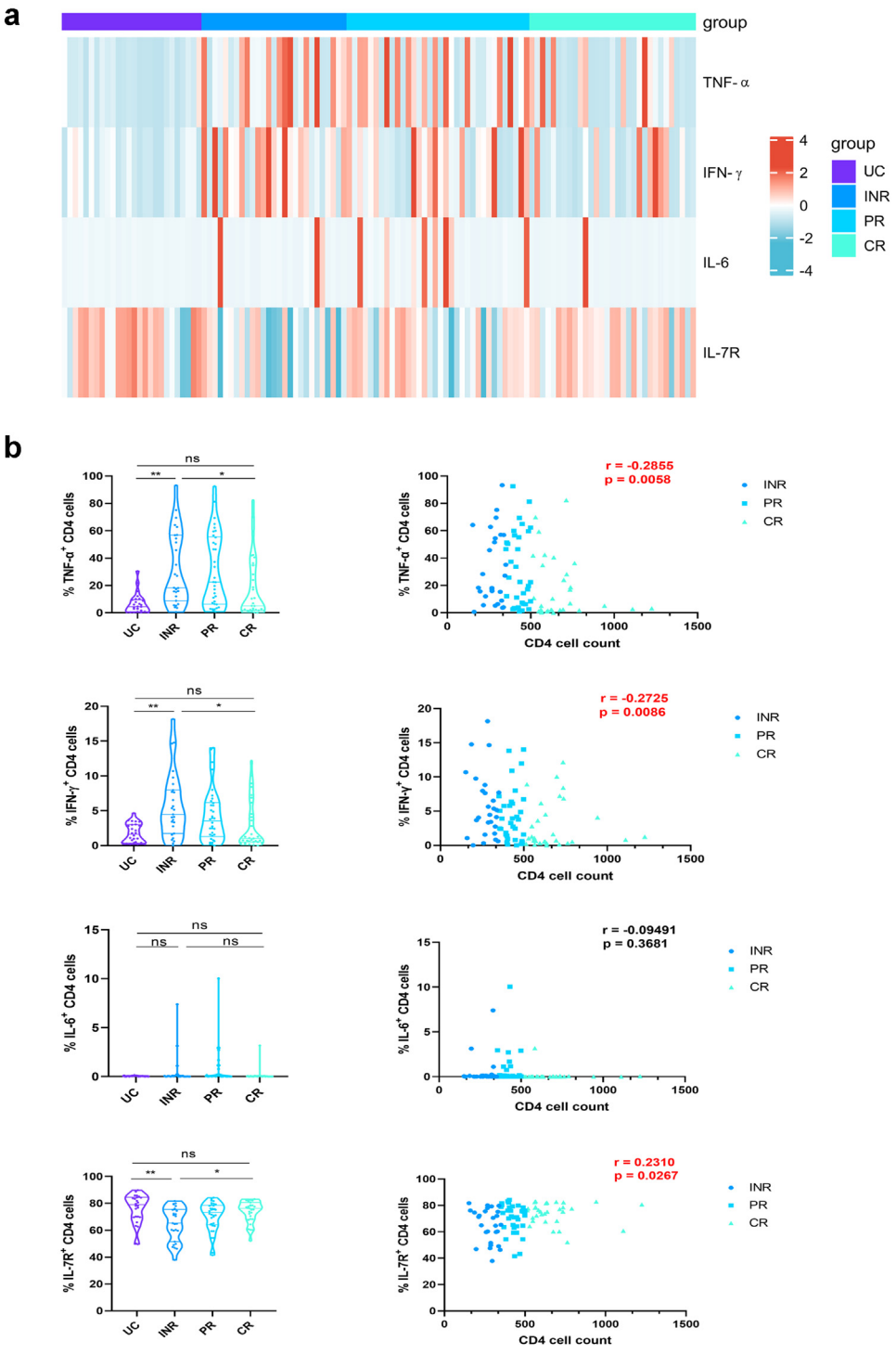

Fig. 4: **Analysis of intracellular cytokines after stimulation and correlations with CD4 cell count in UCs, INRs, PRs, and CRs.** (a) Heatmap of cytokines after stimulation. The percentage of cytokine-producing CD4 cells was expressed as colour scales (blue represents low levels; red represents high levels). The expression of (b) TNF-α, IFN-γ, IL-6, and IL-7R were represented as violin plots comparing median frequency in CD4 cells. And correlation analysis of the percentages of cytokine-producing CD4 cells and CD4 count (UC: n = 26; INR: n = 27, PR: n = 34; CR: n = 31). *p < 0.05, **p < 0.01. UCs, uninfected control participants; INRs, immune non-responders; PRs, partial responders; CRs, complete responders. TNF-α, tumour necrosis factor-α; IFN-γ, interferon-γ; IL-6, interleukin-6; IL-7R, interleukin-7 receptor.

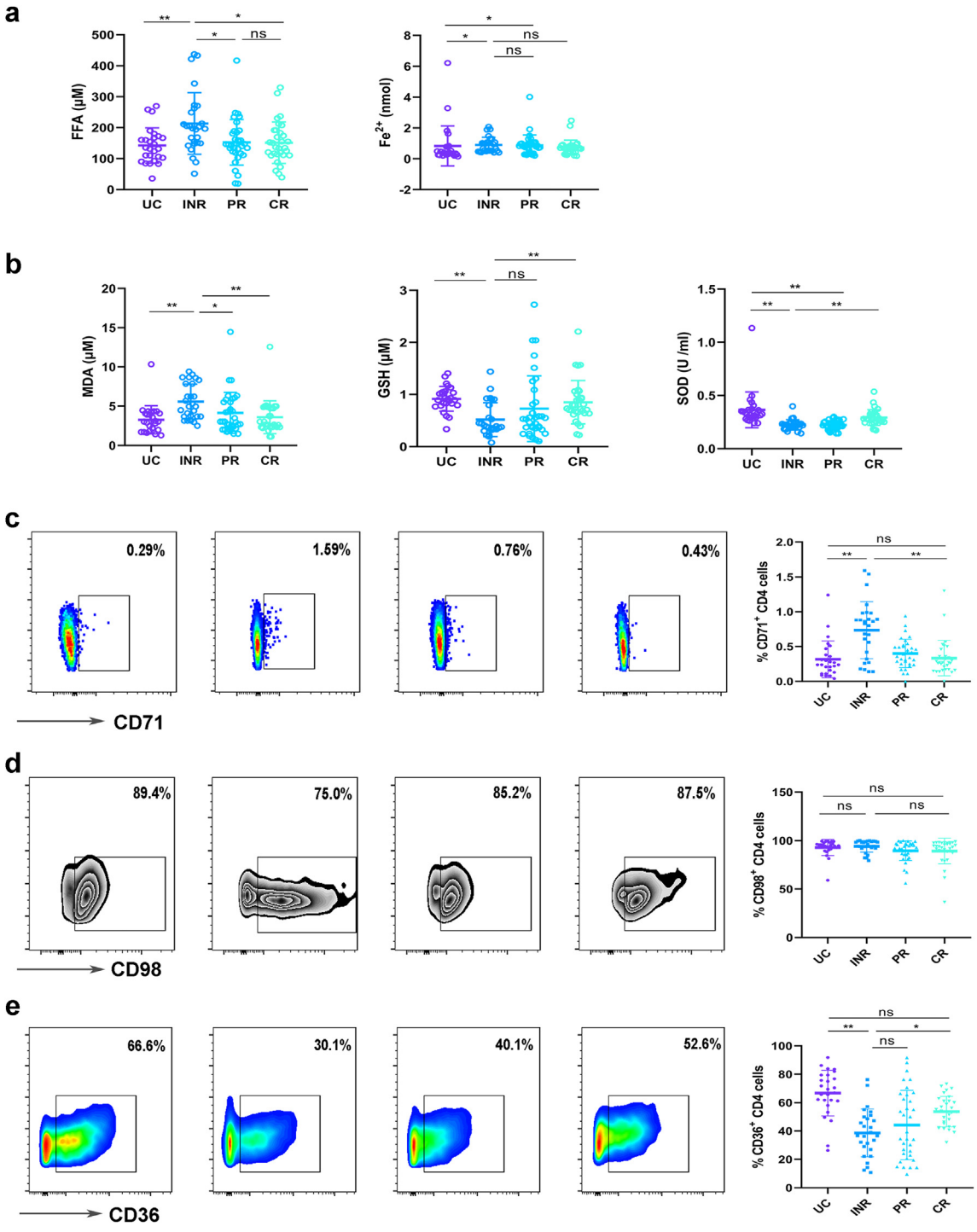

Fig. 5: **Plasma metabolites, oxidative indicators, and metabolic markers on the surface of CD4 cells in UCs, INRs, PRs, and CRs.** (a) The levels of plasma free fatty acid and Fe^{2+}. (b) The oxidative and antioxidant parameters (MDA, GSH, and SOD). And the representative staining (left) and beeswarm boxplots (right) for (c) CD71, (d) CD98, and (e) CD36 on the CD4 cells (UC: n = 26; INR: n = 27, PR: n = 34; CR: n = 31). *p < 0.05, **p < 0.01. UCs, uninfected control participants; INRs, immune non-responders; PRs, partial responders; CRs, complete responders.

CD4 cells are liable to inflammation in INRs

We concurrently measured the expression of cell surface interleukin 7-receptor (IL-7R). After stimulating the cells, we then examined the expression of intracellular inflammatory factors, including TNF-α, IFN-γ, and IL-6. A heatmap of the expression of these factors is represented in Fig. 4a. TNF-α and IFN-γ were significantly higher in INRs than IRs and lower in CRs (Fig. 4b). While not statistically significant, INRs and PRs displayed higher frequencies of IL-6 compared with UCs and CRs. Admittedly, the IL-6 content was extremely low (Fig. 4d), which is because it is secreted later than other cytokines, and 4h stimulation may not induce a high production of IL-6.[37,38] Altogether these data point out that a higher degree of inflammation is seen in INRs compared with UCs and CRs. And the correlation analysis showed a negative association between these factors and CD4 cell count (TNF-α: $r = -0.29$, $p = 0.0058$; IFN-γ: $r = -0.27$, $p = 0.0086$; IL-6: $r = -0.009$, $p = 0.3681$, IL-7R: $r = 0.23$, $p = 0.0267$), supporting the notion of systemic inflammatory dysregulation in PLHIVs contributing to PIR.

Ferroptosis-related metabolism in plasma and CD4 cells in INRs

It has recently been shown that fatty acid saturation and iron ion can modulate ferroptosis sensitivity.[39] Our results found that plasma FFA was significantly higher in INRs, but no significant difference existed between PRs and CRs. Meanwhile, Fe^{2+} did not differ considerably among PLHIVs; but was substantially higher in INRs and PRs than UCs (Fig. 5a). Simultaneously, we measured the plasma MDA, SOD, and GSH, which are metabolites associated with lipid peroxidation. As shown in Fig. 5, MDA was significantly higher in INRs than in the rest three groups, while the antioxidants GSH and SOD were markedly lower in INRs. In contrast, the antioxidant contents of CRs were significantly higher than those of INRs, which were closer to UCs (Fig. 5b).

Ferroptosis is tightly linked to amino acid metabolism, lipid metabolism, and iron metabolism.[19] To determine whether the occurrence of mitochondrial dysfunction and ferroptosis in INRs correlated with these metabolic indicators, we first detected the expression of metabolism markers on the surface of CD4 cells, including transferrin receptor (CD71), amino acid transporter (CD98), and fatty acid transporter (CD36). We found that CD71 expression was higher on the surface of CD4 cells in INRs, compared to PRs and CRs, while the difference was insignificant between CRs and UCs (Fig. 5c). In contrast, CD98 showed almost no difference among the four groups (Fig. 5d). At the same time, CD36 was significantly lower on the surface of CD4 cells in INRs than in the other three groups, and CD36 expression was increased sequentially in PRs and CRs (Fig. 5e). These results suggest that there are iron and lipid metabolism disorders on the surface of CD4 cells in the INRs.

Ferroptosis inhibitors can partially restore mitochondrial functions, reduce inflammatory responses and reverse alterations in metabolic markers in INRs

To verify whether the pathophysiological settings of INRs involve mechanisms and signalling pathways for ferroptosis, ferrostatin-1 (Fer-1), a specific inhibitor of ferroptosis, was utilised. As shown in Fig. 6, when Fer-1 inhibits ferroptosis in the INR, PR, and CR groups, the MMPs were all significantly enhanced within the three groups (Fig. 6a). At the same time, Fer-1 addition could also reduce ROS accumulation and lipid peroxidation to varying degrees in INRs, PRs, and CRs. Of which, Fer-1 has the most substantial improving effect on mitochondrial function in INRs (Fig. 6b and c). Since ferroptosis could amplify inflammation via the release of inflammatory factors into the extracellular environment, we also detected the inflammatory indicators before and after Fer-1 use. We found that TNF-α, IFN-γ, and IL-6 were markedly reduced after Fer-1 intervention (Fig. 6d). It is worth noting that the inflammation-reducing effect of Fer-1 is most pronounced in INRs, as for TNF-α and IFN-γ. Simultaneously, we detected changes in metabolic indicators, and we found that CD71 decreased noticeably, while CD98 and CD36 increased dramatically in PLHIVs after Fer-1 treatment (Fig. 6e). These results demonstrate that ferroptosis inhibitors can reduce the impairment of mitochondrial function and the inflammatory responses of CD4 cells in PLHIVs, especially in INRs.

The ferroptosis-related metabolic indexes were associated with disruption of cellular functions, mitochondrial dysfunction, and inflammation in CD4 cells

The transferrin receptor (CD71) can mediate cellular iron uptake, CD98 is the heavy chain of a neutral amino acid transporter, and CD36 is involved in lipid metabolism and long-chain fatty acid absorption. They are considered nutrition receptors that are essential in cellular metabolism.[40–42] To evaluate the relationships among individual indicators, primarily the metabolism-related indicators with the rest of the functional indices, we did a correlation analysis of each index. We found that CD71 was positively correlated with the activation indicator ($CD38^{+}HLA\text{-}DR^{+}$) ($r = 0.36$, $p = 0.0004$). The amino acid transporter CD98 was negatively correlated with the inflammatory marker IL-6 ($r = -0.3$, $p = 0.0039$), and CD98 was also negatively correlated with CD4 cell killing indicators, including perforin ($r = -0.25$, $p = 0.017$) and granzyme B ($r = -0.33$,

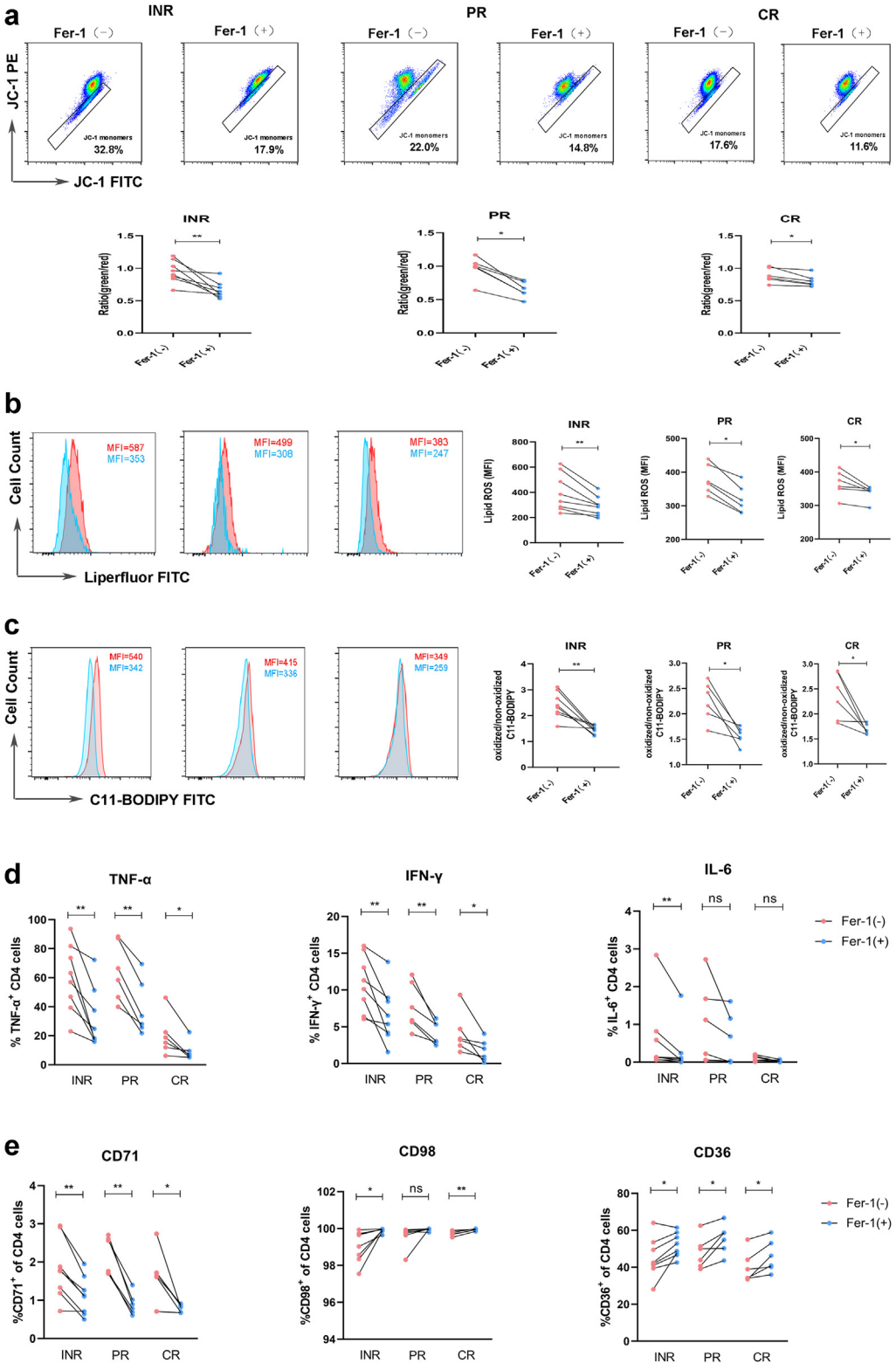

***Fig. 6:* Effect of Fer-1 on mitochondrial functions, inflammatory responses, and metabolic indicators in INRs, PRs, and CRs.** (a) The representative staining (upper) and matching charts (lower) for JC-1 (green/red) within CD4 cells. (b) Intracellular ROS levels were represented as

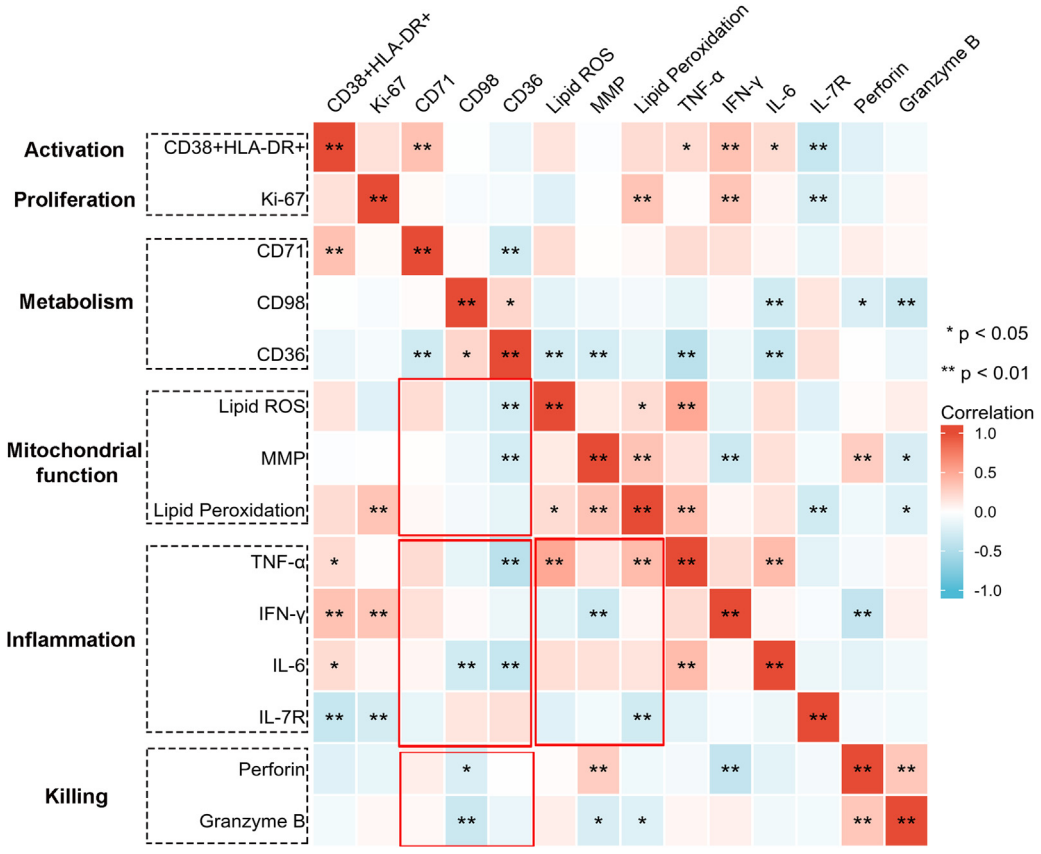

***Fig. 7*: Heatmap of correlation analysis of all individual indicators among CD4 cells in PLHIVs.** The data shown are representative of 92 PLHIVs with 14 complete indicators. The red colour represents a positive correlation; the blue colour represents a negative correlation (UC: n = 26; INR: n = 27, PR: n = 34; CR: n = 31). *p < 0.05, **p < 0.01, and p ≥ 0.05 are not displayed. PLHIVs, people living with HIV.

p = 0.0012). In the meantime, the fatty acid transporter CD36 was negatively correlated with the production of lipid ROS by mitochondria (r = –0.28, p = 0.0067) and the percentage of cells with reduced MMP (r = –0.27, p = 0.0073); CD36 was also negatively correlated with the inflammatory markers TNF-α (r = –0.44, p = 0.00001) and IL-6 (r = –0.36, p = 0.0005) (Fig. 7). In short, metabolic indicators on the surface of CD4 cells were intricately related to mitochondrial function and the inflammatory response. This implies that cellular metabolism may be involved in mitochondrial dysfunction and the inflammatory response.

Discussion

Previous studies have reported that both HIV infection and ART could alter the kinetic function of mitochondria.[43] Moreover, ferroptosis has been widely reported in recent years as a form of cell death characterised by mitochondrial dysfunction and lipid peroxidation, and is associated with various pathophysiological processes and diseases.[44] To explore the functional changes associated with ferroptosis in CD4 cells, we included PLHIVs receiving treatment for more than four years. These patients who showed no significant differences in CD4 cell counts before initiating ART had similarly compromised immune systems at baseline, but showed different immune responses after at least four years of therapy. We then divided them into three groups based on their CD4 cell counts at enrolment: INRs, PRs, and CRs, to unravel the mystery of the development of PIR.

In this study, we observed lowered RTE ($CD45RA^+CD31^+$, TREC), significantly more activated

histograms (left) and matching charts (right). (c) Intracellular lipid peroxidation levels and the ratio of oxidised to non-oxidised C11-BODIPY were represented separately as histograms (left) and matching charts (right). (d) The expression of TNF-α, IFN-γ and IL-6 were represented as matching charts in CD4 cells. (e) The expression of CD71, CD98 and CD36 on the CD4 cells were represented as matching charts (UC: n = 26; INR: n = 27, PR: n = 34; CR: n = 31). *p < 0.05, **p < 0.01. INRs, immune non-responders; PRs, partial responders; CRs, complete responders; TNF-α, tumour necrosis factor-α; IFN-γ, interferon-γ; IL-6, interleukin-6; MFI, median fluorescence intensity.

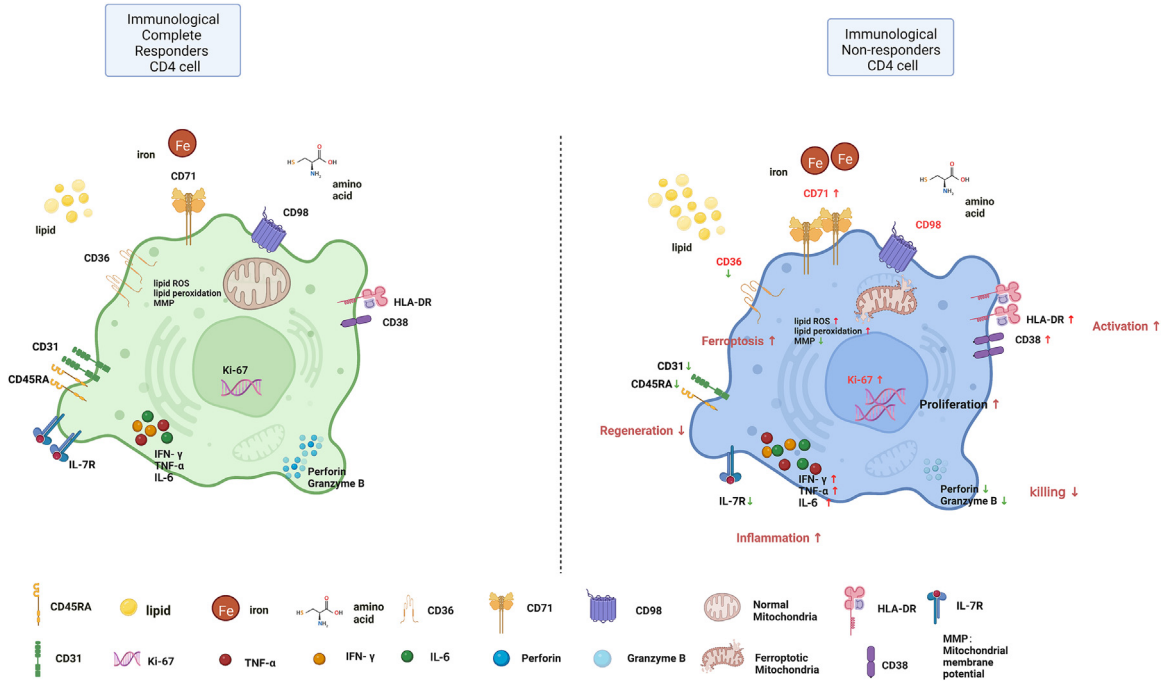

Fig. 8: **Changes in the functional characteristics of CD4 Cells in INRs and CRs.** INRs, immune non-responders; CRs, complete responders.

(HLA-DR$^+$CD38$^+$) and proliferated markers (Ki-67$^+$) but less IL-7R on CD4 cells in INRs, which is consistent with previous studies.[45,46] The RTE expression was directly related to the number of CD4 cells, supporting that RTE is a valuable actor in preserving the homeostasis of the CD4 cell pool. IL-7R expression was negatively linked to CD4 cell hyperactivation and overproliferation. The aberrant immune activation is an essential factor contributing to PIR, and we also found that the activation and proliferation potential of CD4 cells was negatively correlated with immune recovery. In the meantime, CD4 cells have impaired non-specific killing function. CD4 cytotoxic T cells (CTLs) were identified as an unexpected CD4 subset with cytotoxic function by their ability to secrete perforin and granzyme B, and to kill the target cells in an MHC class II-restricted manner.[47] We assume that this type of CD4 cell is damaged in INRs. And the killing functionality of CD4 is positively linked to immune reconstitution. Correlation analysis confirmed a significant positive correlation between the activation and proliferation capacity of the cells and their inflammatory status, which was reported in previous reports.[48,49] It was possible because activated immune cells could secrete a variety of cytokines, chemokines, and inflammatory mediators, leading to severe inflammation and tissue damage.

Since mitochondrial malfunctions and the cumulation of ROS are the hallmark features of ferroptosis, numerous studies have monitored ferroptosis by applying Liperfluor and C11-BODIPY 581/591 dyes to detect cellular lipid peroxidation levels.[50] Bacterial toxins from microbial gut translocation could hamper mitochondrial function, which is frequently linked to increased inflammation through the creation of ROS, a major source of oxidative stress and cell death.[4] The enteric microbiota's enhanced inflammatory characteristics and damage to the gut mucosa with concomitant microbial translocation are the main causes of the chronic inflammation linked to HIV.[51] We then measured levels of ROS, MMP, and lipid peroxides of the total population included. MDA, an ultimate product of lipid peroxidation, was used to assess peroxidative damage, while GSH and SOD, antioxidant enzymes, were used to measure antioxidant levels.[52] We found that plasma and CD4 cell lipid peroxidation damage in INRs was significantly more severe, while the antioxidant barrier was weaker than in PRs and CRs. This indicates that the INRs are in a state of chronic oxidative stress, which harms the recovery of immune function. Accumulation of ROS can impair mitochondria, inducing the collapse of MMP, mitochondrial dysfunction, and ferroptosis. We further found that the MMP of CD4 cells in INRs was significantly reduced compared to UCs, PRs, and CRs. Changes in MMP regulate the activity of essential enzymes in the mitochondria, and MMP reflects the metabolic state of the mitochondria.[53] Structural disruptions often accompany these functional alterations. As shown in Fig. 3, some distinctive ferroptosis changes occur in the morphology of mitochondria in INRs, including loss of structural integrity,

smaller than normal mitochondria, condensation of mitochondrial membrane density, reduction or loss of mitochondrial cristae, and rupture of the outer mitochondrial membrane. Further support for the involvement of ferroptosis comes from the effects of Ferrostatin-1 (Fer-1), employed to elucidate a potential contribution of ferroptosis. Fer-1 can scavenge alkoxyl radicals without being exhausted, combines with Fe^{2+} to reduce unstable iron in cells, scavenges ROS, and thus inhibits lipid peroxidation.[54] Our study found that the aforementioned cell damage and lipid peroxidation in PLHIVs were markedly but not entirely attenuated by Fer-1.

Lipid peroxidation flux may provide a link between inflammation, ferroptosis, and illness,[55] and numerous studies have confirmed that inflammation and iron seem to be tightly regulated, as an inflammatory environment is related to iron accumulation and iron accumulation is linked to a variety of diseases, including neurodegenerative diseases,[56] chronic hepatitis C,[57] tumours,[58] and so on. In our study, we found that the expressions of related inflammatory factors were increased in INRs, including TNF-α, IFN-γ, and IL-6; and the inflammatory state was significantly relieved in CRs. There is no denying that IL-6 levels were markedly lower than TNF-α and IFN-γ. It may be because TNF-α and IFN-γ production begins 1-2 h after stimulation, peaks at approximately 4–6 h, and then declines. In contrast, IL-6 increases significantly at 6 h of stimulation and gradually decreases at 12 and 24 h.[37,38,59] The abundance of IL-6 was still relatively low at the time of the 4 h stimulation. Meanwhile, IL-7R expression was inversely related to ferroptosis markers. Since ferroptosis can initiate inflammation via damage-related model molecules (DAMPs) release, inflammatory diseases may be improved by impeding ferroptosis.[18] We then added ferroptosis inhibitors (Fer-1) and examined the cytokine levels before and after Fer-1 addition, and found that the ferroptosis inhibitor could significantly abate the inflammatory state within CD4 cells. If the inflammatory response exceeds a specific limit, the massive release of proinflammatory cytokines may cause damage to the body.[6] And our results demonstrated that exposure to proinflammatory cytokines was negatively correlated with the restoration of CD4 cells. Therefore, blocking ferroptosis may have significant therapeutic benefits. As ferroptosis fostered inflammation in INRs, and inflammation may conversely act a role in cellular death and destruction mediated by ferroptosis, we speculated that ferroptosis and inflammation could inseparably generate a vicious cycle in INRs, mutually reinforcing and influencing each other.

Iron metabolism, cysteine metabolism, and lipid metabolism can all regulate ferroptosis.[39] The discovery of the transferrin receptor (TFRC, CD71) as a ferroptosis marker also implies that CD71 plays a crucial role in ferroptosis, shedding new light on the mechanism of iron mobilisation during ferroptosis.[60] CD71 can transport exogenous iron ions into the cell by binding to iron storage ferritin, creating an intracellular labile iron pool, which induces the Fenton reaction, leading to the production of ROS.[61] We found Fe^{2+} was higher in INRs and PRs than in UCs, demonstrating a disturbance in iron metabolism in INRs. Meanwhile, CD71 on the surface of CD4 cells was higher than PRs and CRs, which means CD4 cells in INRs can transport more iron ions into the cell. Additionally, increased intracellular iron transport results in an enormous reserve of labile iron in CD4 cells and a higher ROS load. Concurrently, CD71 and CD69 were recently identified as early activation antigens in both human CD4 and CD8 cells.[62] Here, we verified these findings, as we observed that cell-surface expression of CD71 was tightly correlated to $CD38^{+}HLA\text{-}DR^{+}$ (late activation marker) in CD4 cells.

The cystine/glutamate transport system (system xc-) is an essential antioxidant system located in the cell membrane, consisting of two subunits, the light chain SLC7A11 and the heavy chain SLC3A2 (CD98).[63] In our study, we found that the expression of CD98 differed relatively little among groups, suggesting that ferroptosis in CD4 cells may not be mediated by CD98. Despite this, correlation analysis revealed that CD98 expression was negatively correlated with the expression of the inflammatory factor IL-6 and the killing function of CD4 cells, including perforin and granzyme B. Previous studies have reported that nanoparticles containing surface CD98 antibodies and loaded with siCD98 reduced CD98 protein expression on colonic epithelial cells and macrophages and decreased the severity of colitis after oral administration in mice to treat patients with inflammatory bowel disease (IBD).[64] Concurrently, CD98 expression has been reported to be negatively correlated with $CD8^{+}$ T cell characteristics, IFN-γ expression, and patient prognosis in cancer patients.[65] And our study provides support for these reports.

In contrast, CD36 is a scavenger receptor that functions in lipid metabolism and has been reported to induce $CD8^{+}$ T cell ferroptosis via fatty acids metabolism in the tumour microenvironment.[66] In our study, we found that CD36 was markedly decreased on the CD4 cell surface of INRs, while free fatty acids (FFA) were dramatically elevated in INR plasma. Numerous studies have described dyslipidemia in PLHIVs and INRs, especially those with hyperglycemia and thyroid dysfunction, impairing immune recovery,[20,67,68] which is consistent with our findings. Simultaneously, CD36 significantly negatively correlated with CD4 cell mitochondrial function, ferroptosis indicators, and inflammation index. As we know, CD36 controls energy metabolism by recognising long-chain fatty acids (LCFA) and promoting the intracellular accumulation of FFA. If the amount of FFA exceeds the oxidative processing capacity of the mitochondria, the toxic metabolites of FFA accumulate, leading to mitochondrial

dysfunction. And CD36 has been linked to conditions such as insulin resistance, dyslipidemia, diabetes, and atherosclerosis.[69] At the same time, CD36 abnormalities can accelerate the chronic inflammatory response and augment risk factors for inflammatory metabolic diseases.[70,71] These would explain the significance of the correlation between CD36 and other indicators found in Fig. 7. Since CD36 plays a vital role in innate immunity[72–74] and innate immune cells can produce a wide range of inflammatory cytokines,[75] future studies are needed to address the expression of CD36 on innate immune cells and its relationships with other inflammatory factors. There are some discrepancies between our results and those that have been published. Our study found a decrease of CD36 on CD4 cells in INRs, accompanied by an increase in plasma FFA. However, many studies have found that CD36 expression on adipocytes, hepatocytes, and macrophages is increased in patients with hyperlipidemia. Meanwhile, there are also studies that support our findings; studies found that ART caused a significant decrease in CD36 in approximately 70% of participants and that CD36 deficiency caused by continuous ART may lead to insulin resistance and other metabolic complications of steatosis.[76,77] It has also been reported that increased triglycerides and high-density lipoprotein (HDL) levels may be caused by defective CD36-mediated binding of fatty acids and HDL, followed by clearance, which may contribute to lipid abnormalities in CD36 deficiency.[78] And functional studies of CD36 are certainly needed to confirm these findings.

Altogether, the changes in metabolic function were accompanied by mitochondrial morphological and structural changes, typical alterations in cellular ferroptosis, and inflammatory pathways. Ferroptosis inhibitors could notably reverse these changes. The occurrence of immune dysfunction in INRs was the result of the combined effects of these factors. Since there was a close relationship between oxidative stress, ferroptosis, and inflammation, and they may work together and interact with each other; thus it was not certain which factor contributed more. This study explored the possible role of mitochondrial dysfunction and ferroptosis in HIV INRs, and also linked metabolism and ferroptosis to explore further the potential mechanisms associated with PIR, providing new perspectives on the mechanistic study of inadequate immune reconstitution and its treatment. However, there were also some limitations in this study. First, the study was limited by a small sample size and focused only on total CD4 cells but neglected latent viral reservoirs in CD4 cells, so no direct evidence proved that these alterations were HIV-specific responses. Second, the patients enrolled were mainly transmitted through homosexuality, and the gender was predominantly male; some bias may thus exist. Third, there was no knockout or overexpression of the relevant genes. Therefore, further studies with larger sample sizes, including UCs and PLHIVs, are required to determine the relationship between cellular metabolism and its functions in diverse innate and adaptive immune cells. And further validation and more in-depth research are warranted in future studies. We will continue to explore further the specific molecular mechanisms of CD36 involvement in lipid metabolism-regulated ferroptosis in INRs, in an attempt to find either a direct target or a pathway for its action.

Contributors

Study Design, QX, FTY and FJZ; Clinical Sample Collection, QX, FTY, LTY, JX, QL, and XJL; Experimental implementation, QX, FTY, LTY and YSS; Methodology, QX, FTY, JYH and YXT; Data curation, QX, LTY, ZC and QL; Project administration, HXZ and FJZ; Software, SYY and YXT; Visualization, FTY, JYH and FJZ; Writing-original draft, QX; Writing-review & editing, FTY and JYH. QX, LTY, ZC and QL had direct access and verified the underlying study data. The corresponding authors, FTY and FJZ, had full access to all the data and had final responsibility for the decision to submit it for publication. All authors provided intellectual input and have read and approved the final version of the manuscript.

Data sharing statement

The raw data supporting the conclusions of this article will be made available by the authors without undue reservation.

Declaration of interests

The authors declare no conflict of interest.

Acknowledgements

The authors would like to acknowledge Beijing Ditan Hospital, Capital Medical University, and the Beijing Key Laboratory of Emerging Infectious Disease to support the study. The authors thank Ke Chang and Zhennan Li of the Beijing Ditan Hospital Red Ribbon Home for their help in patient recruitment, and Professor Hui Zeng and Professor Chen Chen of the Beijing Shijitan Hospital Affiliated to Capital Medical University for their help in research optimisation. Simultaneously, the authors sincerely thank Professor Cheng Yang of Chongqing Key Laboratory of Infectious and Parasitic Diseases for his guidance on flow cytometry experimental techniques, and Jiaqi Lu and Leidan Zhang of Beijing Institute of Infectious Diseases for their aid in flow cytometry results analysis.

We also thank our funding sources, including the 13th Five-year Plan, Ministry of Science and Technology of China (2018ZX10302-102), Beijing Municipal Administration of Hospitals' Ascent Plan (DFL20191802), and Beijing Municipal Administration of Hospitals Clinical Medicine Development of Special Funding Support (ZYLX202126).

Appendix A. Supplementary data

Supplementary data related to this article can be found at https://doi.org/10.1016/j.ebiom.2022.104382.

References

1 Ramirez CM, Sinclair E, Epling L, et al. Immunologic profiles distinguish aviremic HIV-infected adults. *Aids*. 2016;30(10):1553–1562.

2 Bartlett J. *Panel on Antiretroviral Guidelines for Adults and Adolescents. Guidelines for the use of antiretroviral agents in HIV-1-infected adults and adolescents*. Washington, D.C.: The Department of

Health and Human Services Panel on Antiretroviral Guidelines for Adult and Adolescents; 2008:1–128.
3 Shukla S, Kumari S, Bal SK, et al. "Go", "No Go," or "Where to Go"; does microbiota dictate T cell exhaustion, programming, and HIV persistence? *Curr Opin HIV AIDS*. 2021;16(4):215–222.
4 Ferrari B, Da Silva AC, Liu KH, et al. Gut-derived bacterial toxins impair memory CD4+ T cell mitochondrial function in HIV-1 infection. *J Clin Invest*. 2022;132(9):e149571.
5 Younes SA, Yassine-Diab B, Dumont AR, et al. HIV-1 viremia prevents the establishment of interleukin 2-producing HIV-specific memory CD4+ T cells endowed with proliferative capacity. *J Exp Med*. 2003;198(12):1909–1922.
6 Yang X, Su B, Zhang X, Liu Y, Wu H, Zhang T. Incomplete immune reconstitution in HIV/AIDS patients on antiretroviral therapy: Challenges of immunological non-responders. *J Leukoc Biol*. 2020;107(4):597–612.
7 Carvalho-Silva WHV, Andrade-Santos JL, Souto FO, Coelho AVC, Crovella S, Guimarães RL. Immunological recovery failure in cART-treated HIV-positive patients is associated with reduced thymic output and RTE CD4+ T cell death by pyroptosis. *J Leukoc Biol*. 2020;107(1):85–94.
8 Saag MS, Benson CA, Gandhi RT, et al. Antiretroviral drugs for treatment and prevention of HIV infection in adults: 2018 recommendations of the International Antiviral Society-USA Panel. *JAMA*. 2018;320(4):379–396.
9 Prabhu S, Harwell JI, Kumarasamy N. Advanced HIV: diagnosis, treatment, and prevention. *Lancet HIV*. 2019;6(8):e540–e551.
10 Cunningham CA, Helm EY, Fink PJ. Reinterpreting recent thymic emigrant function: defective or adaptive? *Curr Opin Immunol*. 2018;51:1–6.
11 Rubio A, Martínez-Moya M, Leal M, et al. Changes in thymus volume in adult HIV-infected patients under HAART: correlation with the T-cell repopulation. *Clin Exp Immunol*. 2002;130(1):121–126.
12 Stockwell BR, Friedmann Angeli JP, Bayir H, et al. Ferroptosis: a regulated cell death nexus linking metabolism, redox biology, and disease. *Cell*. 2017;171(2):273–285.
13 Gan B. Mitochondrial regulation of ferroptosis. *J Cell Biol*. 2021;220(9).
14 Agmon E, Stockwell BR. Lipid homeostasis and regulated cell death. *Curr Opin Chem Biol*. 2017;39:83–89.
15 Nakamura T, Naguro I, Ichijo H. Iron homeostasis and iron-regulated ROS in cell death, senescence and human diseases. *Biochim Biophys Acta Gen Subj*. 2019;1863(9):1398–1409.
16 Ham 3rd PB, Raju R. Mitochondrial function in hypoxic ischemic injury and influence of aging. *Prog Neurobiol*. 2017;157:92–116.
17 Dixon SJ, Lemberg KM, Lamprecht MR, et al. Ferroptosis: an iron-dependent form of nonapoptotic cell death. *Cell*. 2012;149(5):1060–1072.
18 Yoshida M, Minagawa S, Araya J, et al. Involvement of cigarette smoke-induced epithelial cell ferroptosis in COPD pathogenesis. *Nat Commun*. 2019;10(1):3145.
19 Stockwell BR, Jiang X, Gu W. Emerging mechanisms and disease relevance of ferroptosis. *Trends Cell Biol*. 2020;30(6):478–490.
20 Beraldo RA, Santos APD, Guimarães MP, et al. Body fat redistribution and changes in lipid and glucose metabolism in people living with HIV/AIDS. *Rev Bras Epidemiol*. 2017;20(3):526–536.
21 Jiang X, Stockwell BR, Conrad M. Ferroptosis: mechanisms, biology and role in disease. *Nat Rev Mol Cell Biol*. 2021;22(4):266–282.
22 Agmon E, Solon J, Bassereau P, Stockwell BR. Modeling the effects of lipid peroxidation during ferroptosis on membrane properties. *Sci Rep*. 2018;8(1):5155.
23 Kajarabille N, Latunde-Dada GO. Programmed cell-death by ferroptosis: antioxidants as mitigators. *Int J Mol Sci*. 2019;20(19):4968.
24 Cao D, Khanal S, Wang L, et al. A matter of life or death: productively infected and bystander CD4 T cells in early HIV infection. *Front Immunol*. 2020;11:626431.
25 Xu X, Lin D, Tu S, Gao S, Shao A, Sheng J. Is ferroptosis a future direction in exploring cryptococcal meningitis? *Front Immunol*. 2021;12:598601.
26 Sfera A, Thomas KG, Andronescu CV, et al. Bromodomains in human-immunodeficiency virus-associated neurocognitive disorders: a model of ferroptosis-induced neurodegeneration. *Front Neurosci*. 2022;16:904816.
27 Subashini D, Dinesha TR, Srirama RB, et al. Mitochondrial DNA content of peripheral blood mononuclear cells in ART untreated & stavudine/zidovudine treated HIV-1-infected patients. *Indian J Med Res*. 2018;148(2):207–214.
28 Perrin S, Cremer J, Roll P, et al. HIV-1 infection and first line ART induced differential responses in mitochondria from blood lymphocytes and monocytes: the ANRS EP45 "Aging" study. *PLoS One*. 2012;7(7):e41129.
29 Yu F, Hao Y, Zhao H, et al. Distinct mitochondrial disturbance in CD4+T and CD8+T cells from HIV-infected patients. *J Acquir Immune Defic Syndr*. 2017;74(2):206–212.
30 Iannetti EF, Willems PH, Pellegrini M, et al. Toward high-content screening of mitochondrial morphology and membrane potential in living cells. *Int J Biochem Cell Biol*. 2015;63:66–70.
31 Zhang LX, Song JW, Zhang C, et al. Dynamics of HIV reservoir decay and naïve CD4 T-cell recovery between immune non-responders and complete responders on long-term antiretroviral treatment. *Clin Immunol*. 2021;229:108773.
32 Mold JE, Réu P, Olin A, et al. Cell generation dynamics underlying naive T-cell homeostasis in adult humans. *PLoS Biol*. 2019;17(10):e3000383.
33 Li H, Adamopoulos IE, Moulton VR, et al. Systemic lupus erythematosus favors the generation of IL-17 producing double negative T cells. *Nat Commun*. 2020;11(1):2859.
34 Korsunskiy I, Blyuss O, Gordukova M, et al. Expanding TREC and KREC utility in primary immunodeficiency diseases diagnosis. *Front Immunol*. 2020;11:320.
35 Basu R, Huse M. Mechanical communication at the immunological synapse. *Trends Cell Biol*. 2017;27(4):241–254.
36 Buck MD, O'Sullivan D, Klein Geltink RI, et al. Mitochondrial dynamics controls T cell fate through metabolic programming. *Cell*. 2016;166(1):63–76.
37 Sohlberg E, Saghafian-Hedengren S, Bremme K, Sverremark-Ekström E. Cord blood monocyte subsets are similar to adult and show potent peptidoglycan-stimulated cytokine responses. *Immunology*. 2011;133(1):41–50.
38 Huang L, Ma Q, Li Y, Li B, Zhang L. Inhibition of microRNA-210 suppresses pro-inflammatory response and reduces acute brain injury of ischemic stroke in mice. *Exp Neurol*. 2018;300:41–50.
39 Lang X, Green MD, Wang W, et al. Radiotherapy and immunotherapy promote tumoral lipid oxidation and ferroptosis via synergistic repression of SLC7A11. *Cancer Discov*. 2019;9(12):1673–1685.
40 Montemiglio LC, Testi C, Ceci P, et al. Cryo-EM structure of the human ferritin-transferrin receptor 1 complex. *Nat Commun*. 2019;10(1):1121.
41 Loftus RM, Assmann N, Kedia-Mehta N, et al. Amino acid-dependent cMyc expression is essential for NK cell metabolic and functional responses in mice. *Nat Commun*. 2018;9(1):2341.
42 Pietka TA, Schappe T, Conte C, et al. Adipose and muscle tissue profile of CD36 transcripts in obese subjects highlights the role of CD36 in fatty acid homeostasis and insulin resistance. *Diabetes Care*. 2014;37(7):1990–1997.
43 Blas-Garcia A, Apostolova N, Esplugues JV. Oxidative stress and mitochondrial impairment after treatment with anti-HIV drugs: clinical implications. *Curr Pharm Des*. 2011;17(36):4076–4086.
44 Feng H, Stockwell BR. Unsolved mysteries: how does lipid peroxidation cause ferroptosis? *PLoS Biol*. 2018;16(5):e2006203.
45 Paiardini M, Müller-Trutwin M. HIV-associated chronic immune activation. *Immunol Rev*. 2013;254(1):78–101.
46 Rajasuriar R, Booth D, Solomon A, et al. Biological determinants of immune reconstitution in HIV-infected patients receiving antiretroviral therapy: the role of interleukin 7 and interleukin 7 receptor α and microbial translocation. *J Infect Dis*. 2010;202(8):1254–1264.
47 Takeuchi A, Saito T. CD4 CTL, a cytotoxic subset of CD4(+) T cells, their differentiation and function. *Front Immunol*. 2017;8:194.
48 Zhang C, Song JW, Huang HH, et al. NLRP3 inflammasome induces CD4+ T cell loss in chronically HIV-1-infected patients. *J Clin Invest*. 2021;131(6).
49 Doitsh G, Galloway NL, Geng X, et al. Cell death by pyroptosis drives CD4 T-cell depletion in HIV-1 infection. *Nature*. 2014;505(7484):509–514.
50 Verma N, Vinik Y, Saroha A, et al. Synthetic lethal combination targeting BET uncovered intrinsic susceptibility of TNBC to ferroptosis. *Sci Adv*. 2020;6(34).
51 Morou A, Brunet-Ratnasingham E, Dubé M, et al. Altered differentiation is central to HIV-specific CD4(+) T cell dysfunction in progressive disease. *Nat Immunol*. 2019;20(8):1059–1070.
52 Chen M, Yan XT, Ye L, Tang JJ, Zhang ZZ, He XH. Dexmedetomidine ameliorates lung injury induced by intestinal ischemia/reperfusion by upregulating cannabinoid receptor 2, followed by the activation of the phosphatidylinositol 3-kinase/akt pathway. *Oxid Med Cell Longev*. 2020;2020:6120194.

53 Arfaoui A, El Hadrami A, Daayf F. Pre-treatment of soybean plants with calcium stimulates ROS responses and mitigates infection by Sclerotinia sclerotiorum. *Plant Physiol Biochem*. 2018;122:121–128.
54 Miotto G, Rossetto M, Di Paolo ML, et al. Insight into the mechanism of ferroptosis inhibition by ferrostatin-1. *Redox Biol*. 2020;28:101328.
55 Markar SR, Wiggins T, Antonowicz S, et al. Assessment of a noninvasive exhaled breath test for the diagnosis of oesophagogastric cancer. *JAMA Oncol*. 2018;4(7):970–976.
56 Fernández-Mendívil C, Luengo E, Trigo-Alonso P, García-Magro N, Negredo P, López MG. Protective role of microglial HO-1 blockade in aging: implication of iron metabolism. *Redox Biol*. 2021;38:101789.
57 Corengia C, Galimberti S, Bovo G, et al. Iron accumulation in chronic hepatitis C: relation of hepatic iron distribution, HFE genotype, and disease course. *Am J Clin Pathol*. 2005;124(6):846–853.
58 Vela D. Iron in the tumor microenvironment. *Adv Exp Med Biol*. 2020;1259:39–51.
59 Iftakhar EKI, Koide N, Hassan F, et al. Novel mechanism of U18666A-induced tumour necrosis factor-alpha production in RAW 264.7 macrophage cells. *Clin Exp Immunol*. 2009;155(3):552–558.
60 Feng H, Schorpp K, Jin J, et al. Transferrin receptor is a specific ferroptosis marker. *Cell Rep*. 2020;30(10):3411–3423.e7.
61 Tang D, Kang R, Berghe TV, Vandenabeele P, Kroemer G. The molecular machinery of regulated cell death. *Cell Res*. 2019;29(5):347–364.
62 Starska K, Głowacka E, Kulig A, Lewy-Trenda I, Bryś M, Lewkowicz P. Prognostic value of the immunological phenomena and relationship with clinicopathological characteristics of the tumor–the expression of the early CD69+, CD71+ and the late CD25+, CD26+, HLA/DR+ activation markers on T CD4+ and CD8+ lymphocytes in squamous cell laryngeal carcinoma. Part II. *Folia Histochem Cytobiol*. 2011;49(4):593–603.
63 Buckingham SC, Campbell SL, Haas BR, et al. Glutamate release by primary brain tumors induces epileptic activity. *Nat Med*. 2011;17(10):1269–1274.
64 Xiao B, Laroui H, Viennois E, et al. Nanoparticles with surface antibody against CD98 and carrying CD98 small interfering RNA reduce colitis in mice. *Gastroenterology*. 2014;146(5):1289–1300.e1-19.
65 Wang W, Green M, Choi JE, et al. CD8(+) T cells regulate tumour ferroptosis during cancer immunotherapy. *Nature*. 2019;569(7755):270–274.
66 Ma X, Xiao L, Liu L, et al. CD36-mediated ferroptosis dampens intratumoral CD8(+) T cell effector function and impairs their antitumor ability. *Cell Metab*. 2021;33(5):1001–1012.e5.
67 Ji S, Xu Y, Han D, et al. Changes in lipid indices in HIV+ cases on HAART. *Biomed Res Int*. 2019;2019:2870647.
68 Qian S, Chen X, Wu T, et al. The accumulation of plasma acylcarnitines are associated with poor immune recovery in HIV-infected individuals. *BMC Infect Dis*. 2021;21(1):808.
69 Silverstein RL, Febbraio M. CD36, a scavenger receptor involved in immunity, metabolism, angiogenesis, and behavior. *Sci Signal*. 2009;2(72):re3.
70 Zhao L, Zhang C, Luo X, et al. CD36 palmitoylation disrupts free fatty acid metabolism and promotes tissue inflammation in non-alcoholic steatohepatitis. *J Hepatol*. 2018;69(3):705–717.
71 Febbraio M, Hajjar DP, Silverstein RL. CD36: a class B scavenger receptor involved in angiogenesis, atherosclerosis, inflammation, and lipid metabolism. *J Clin Invest*. 2001;108(6):785–791.
72 Wang J, Li Y. CD36 tango in cancer: signaling pathways and functions. *Theranostics*. 2019;9(17):4893–4908.
73 Kanoke A, Nishijima Y, Ljungberg M, et al. The effect of type 2 diabetes on CD36 expression and the uptake of oxLDL: diabetes affects CD36 and oxLDL uptake. *Exp Neurol*. 2020;334:113461.
74 Rayasam A, Mottahedin A, Faustino J, Mallard C, Vexler ZS. Scavenger receptor CD36 governs recruitment of myeloid cells to the blood-CSF barrier after stroke in neonatal mice. *J Neuroinflammation*. 2022;19(1):47.
75 Luo L, Bokil NJ, Wall AA, et al. SCIMP is a transmembrane non-TIR TLR adaptor that promotes proinflammatory cytokine production from macrophages. *Nat Commun*. 2017;8:14133.
76 Serghides L, Nathoo S, Walmsley S, Kain KC. CD36 deficiency induced by antiretroviral therapy. *AIDS*. 2002;16(3):353–358.
77 Yanai H, Chiba H, Morimoto M, et al. Human CD36 deficiency is associated with elevation in low-density lipoprotein-cholesterol. *Am J Med Genet*. 2000;93(4):299–304.
78 Furuhashi M, Ura N, Nakata T, Shimamoto K. Insulin sensitivity and lipid metabolism in human CD36 deficiency. *Diabetes Care*. 2003;26(2):471–474.